17th World Conference on Earthquake Engineering, 17WCEE
Sendai, Japan - September 13th to 18th 2020
Paper N° C003460
Registration Code: S-A00279

LONG-TERM VIBRATION EXPERIMENT OF A BASE-ISOLATED BUILDING

J. Tobita[(1)], N. Fukuwa[(2)]

[(1)] Professor, Nagoya University, tobita@nagoya-u.jp
[(2)] Professor, Nagoya University, fukuwa@nagoya-u.jp

Abstract

Using an actual size base-isolated building, various vibration experiments have continuously done in 5 years and change and fluctuation of vibration characteristics are examined. Identification of stiffness, friction coefficient and damping coefficient of isolation devices are also tried.

The building named “The Gensaikan” is four-story reinforced concrete structure of distinguished triangular shape with approximately 3,000 m^2 floor area and 5,600 t weight. The base-isolation system is consists of 5 natural rubber bearings, 9 cross linear bearings and 8 oil dampers, devices are showing approximately linear elastic properties. Fundamental natural period of the building is designed as 5.2 s, which is much longer than the site predominant period of 2.6 s. The clearance of base-isolated layer is 90 cm.

Two types of vibration facilities are equipped permanently to ensure regular experiments at an actual building. One is a free vibration test devices at basement floor, newly developed three oil jacks of 100 t force each to make initial displacement of 150mm. The other is a forced vibration test by shaking a laboratory room of 410 t weight on the rooftop isolated by cross linear bearings and rubber bearings. The room is able to shake by electric actuators up to 70 cm with period of 5 s. It is possible to produce an internal force of 40 t by shaking the room, which causes approximately 5 cm relative displacement of the 5,600 t main building. The laboratory loom is also used for vibration experience of ling-period building responses. These two types of vibration experiments have done over 100 times in 5 years.

The building is equipped with several seismometers, relative displacement gauges, strain gauges and earth pressure gauges on the basement. They can be used for understanding the vibrational behavior of the building during experiments, changes in the building and the isolation system over time, and the distribution characteristics of earth pressure during earthquakes. Earthquake response and ambient vibration are also observed.

Observed natural frequencies and damping ratios are stable in 5 years, and a slight dependency of temperature and amplitude are shown. Elastic stiffness and damping of rubber bearings, friction coefficient of cross linear bearings, and damping coefficient of oil dampers are identified by using vibration experiment responses. Estimated values fluctuate to some extent, however they are consistent with design values. Damping force of each oil damper is now tried to measure using strain gauges. Based on the accumulated data, it is possible to continuously examine the performance of the seismic isolation device in the actual building, over a long period of time.

Keywords: base-isolation; vibration experiment; change of vibration characteristics; identification; observation

1. Introduction

The Nagoya University Disaster Mitigation Research Building, henceforth "subject building," used as the subject for the current study is a base-isolated building with a laboratory on the roof, which is capable of excitation using an isolation device. The building itself is designed to handle various vibration tests. Two types of vibration tests, free and forced vibration tests using permanent loading equipment, can be conducted, and it is distinct in that the response characteristics including the influence of environmental conditions and changes over time of the existing building can be repeatedly investigated over long periods of time at the building-scale with high-density measurement systems including those for ground response and earth pressure. The present research analyzes the response and isolation device characteristics of a base-isolated building based on vibration tests.

2. Subject Site and Building

The subject building, shown in Fig.1, is a base-isolated building with RC footing, comprised of four aboveground floors and one rooftop laboratory floor. The isolated layer is belowground and is enclosed by three retaining walls excluding the north side. The isolation device used five laminated natural rubber isolators, henceforth, "rubber bearing," nine cross linear bearings, "CLB," and eight oil dampers, and the device was designed to show base-isolated building behavior from a relatively low amplitude by making the initial stiffness smaller with linearly elastic restoring force characteristics. The superstructure is approximately 5,900 tons, the isolated natural period of the whole building was set to 5.2 s, and the equivalent damping coefficient was set to 0.31 because the dominant period during the long period range originating from the deeper ground structure of the building was approximately 3 s.

The rooftop laboratory is supported by isolation device as shown in Fig.2. The structure is approximately 400 tons, and supported using four CLBs and four laminated rubber bearings. The natural period of the rooftop isolated layer was set to 5.2 s in accordance with the natural period of the base-isolated foundation layer. The rooftop isolated layer is usually fixed with a shear pin.

Fig.1 Subject building

Fig.2 Rooftop laboratory

3. Vibration Tests and Measurement Environment

3.1 Free vibration test

A total of three hydraulic jacks as shown in Fig.3, each with a performance of 1000 kN, are permanently placed in the base-isolated foundation layer of the subject building to conduct free vibration tests. An initial displacement is applied to the main building body by pulling on it using hydraulic jacks, and its release results in a response in the direction away from the jack due to the restoring force of the isolation device,

thereby exciting the free vibration of the main building body. Such an experiment is possible because the isolation device of the subject building has almost entirely elastic restoring force characteristics with small initial stiffness values. Numerous free vibration tests of base-isolated buildings have applied an initial displacement by pushing with a quick-release jack, but a low-cost permanent jack for use in free vibration tests was newly designed because of the continuous nature of the conducted tests, and the validity of this method was confirmed[1, 2].

3.2 Forced vibration test

The rooftop laboratory can be vibrated using an electric actuator as shown in Fig.4. The maximum force capability of the actuator is relatively low at approximately 80 kN, but large vibrations can be induced with resonance using stationary vibrations that correspond with the natural period of the rooftop isolated layer. Additionally, the natural period can be shortened by restricting the lower stage of the double-staged laminated rubber in the rooftop isolated layer. The main building body also vibrates because of the excitation of the rooftop laboratory, and a forced vibration test of the entire building is possible.

3.3 Measurement

The subject building has accelerometers at ten locations, the base-isolated foundation layer has two relative displacement meters in two directions, and the retaining walls of the isolated layer has four earth pressure gages, all permanently placed, and is an environment in which measurements can be made during earthquakes and vibration tests. The placements of the measuring instruments are shown in Fig.5.

Additionally, strain gages were newly set up on the rods of eight oil dampers in the base-isolated foundation layer in addition to the permanently placed measuring instruments to analyze the damping characteristics of the oil damper during vibration tests.

Fig.3 Hydraulic jack (blue)

Fig.4 Electric actuator (red)

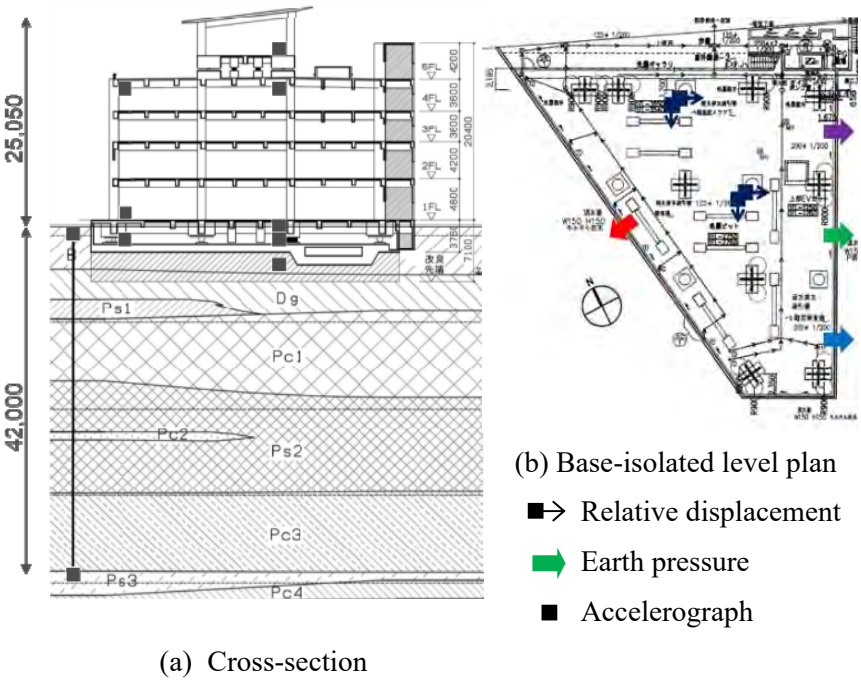

Fig.5 Building outline and response measurement sensors

4. Vibration Characteristics of the Base-Isolated Building Based on Vibration Tests

4.1 Free vibration tests

Measurement records of the free vibration test are shown in Fig.5. The displacement records showed a response with no vibration that was asymptotic to a neutral point in cases where Fig.5(a) the oil damper was present, and it is predicted that damping due to the oil dampers is large. Additionally, although experimental variation was present, residual deformation of approximately 1 cm occurred. Vibrations occurred in cases where Fig.5(b) the oil damper was not present and residual deformation relative to (a) was low.

Identification of the base-isolated foundation layer waveform was conducted using the damped elastic vibration equation with the natural period and damping coefficient during the free vibration tests[3]. Identification results are summarized in Table 1, and the identified waveforms are shown in Fig.6. The identified waveforms showed a virtually identical match with measured waveforms when (a) the oil damper was present, whereas the modeled and measured waveforms were only aligned in the range where high displacement was observed during vibration and not in the range with low amplitude when (b) the oil damper was not present. This was thought to be due to the influence of friction from CLB in the base-isolated foundation layer, which was not factored into the single-degree-of-freedom (SDOF) viscous damping model.

The modeled natural periods for both (a) and (b) were shorter than the designated period of 5.2 s. The natural periods during both low-amplitude and high-amplitude periods are expected to be the same due to the fact that the restoring force characteristics of the isolated layer of the subject building were designed so that they are almost entirely elastic, but it is thought that the influence of friction from CLB in the base-isolated layer had become relatively large under small amplitude values of approximately 140 mm in the free vibration tests, and the isolated period became shorter as a result.

The damping coefficient modeled in (a) was over 0.80 and was two times greater than the 0.31 value of the equivalent viscous damping coefficient, corresponding to four oil dampers. This was thought to be due to the fact that the damping force of oil dampers is bilinear with regards to velocity, and that it is influenced by an increased damping force when the velocity is below the relief rate. The damping coefficient modeled in (b) became smaller as the initial displacement increased, and the vibration characteristics exhibited a dependency to amplitude.

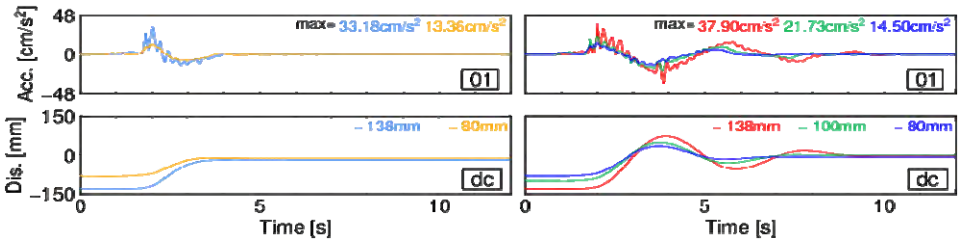

Fig.5(a) Free vibration with oil dampers

Fig5(b) Free vibration without oil dampers

Table 1(a) Estimated parameters with oil dampers

Initial disp.	Initial vel.	Natural period	Damping
138 mm	2.95 cm/s	4.58 s	0.84
80 mm	1.19 cm/s	4.04 s	0.82

Table 1(b) Estimated parameters without oil dampers

Initial disp.	Initial vel.	Natural period	Damping
138 mm	6.28 cm/s	4.39 s	0.27
100 mm	4.70 cm/s	4.01 s	0.21
80 mm	2.80 cm/s	3.95 s	0.16

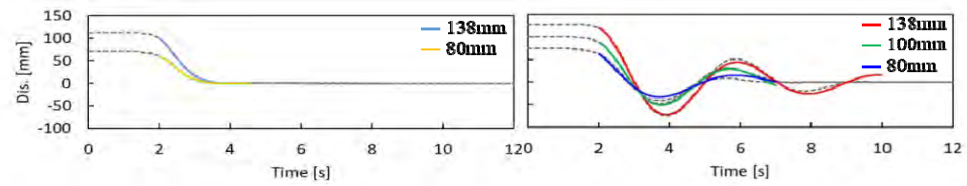

Fig.6(a) Identified free vibration with dampers

Fig.6(b) Identified free vibration without dampers

4.2 Forced vibration tests

The measurement records of the forced vibration tests are shown in Fig.7. The building acceleration rate began to increase after the rooftop acceleration rate surpassed approximately 50 cm/s^2, and the acceleration rate of the building was thought to have exceeded the static friction of the base-isolated foundation layer, resulting in a larger response.

Additionally, the acceleration Fourier spectra at each measurement point were prominent at frequency values that were multiples of the excitation frequency. Excitations due to the response of the rooftop laboratory, which was the vibration source as the controlled actuator, and the rocking of the rooftop laboratory during testing were thought to have been influenced. This was additionally thought to have been a distinct response characteristic of the forced vibration tests.

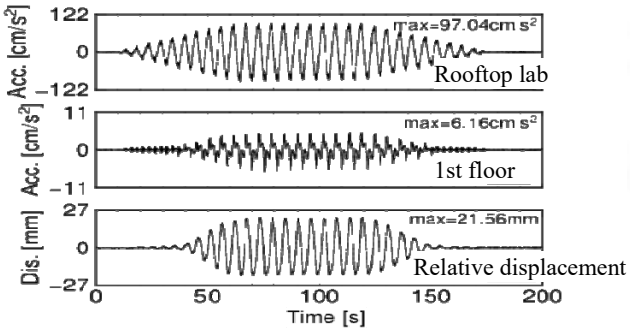

Fig.7(a) Observed response during forced vibration

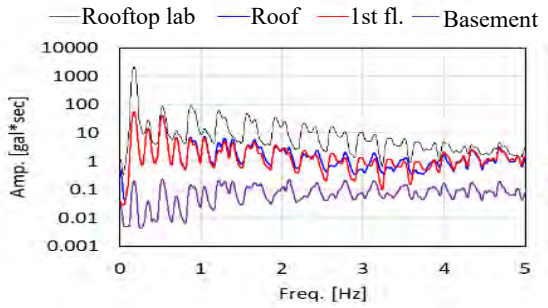

Fig.7(b) Fourier spectra for acceleration response

5. Characteristics of Base-Isolated Devices Based on Vibration Tests

5.1 Horizontal stiffness and friction of the base-isolated layer based on static loading

The load-displacement relationship of the base-isolated layer obtained from static loading tests is shown in Fig.8. The slope corresponds to the horizontal stiffness of the base-isolated layer, and the intercept corresponds to friction. The stiffness and friction, both determined from least squares-based linear approximation, are shown in Fig.9. The designated stiffness value of the five rubber bearings in the base-isolated layer is 9.21 kN/mm. The stiffness of the laminated rubber bearing is known to depend on surface pressure and shearing strain, and both the stiffness value that incorporates these factors based on factory experimental test data of devices, shown as dashed line in Fig.9, and the stiffness value of the base-isolated layer are equivalent. Additionally, the friction of the base-isolated layer and the friction of CLB, determined from the product of the CLB friction coefficient 0.0039 and the total axial force borne by the nine CLB units 4,220 tons, are larger than factory experimental data 161.5 kN. Most of the friction in the base-isolated layer is that of CLB but may also include interference from setups with expansion joints and other equipment.

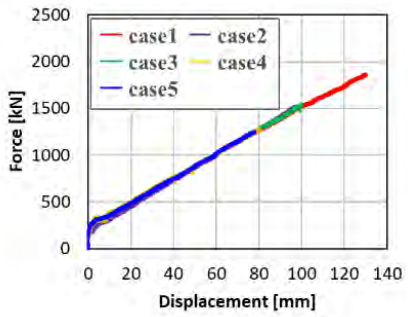

Fig.8 Load-displacement relationship of base-isolated layer from static loading test

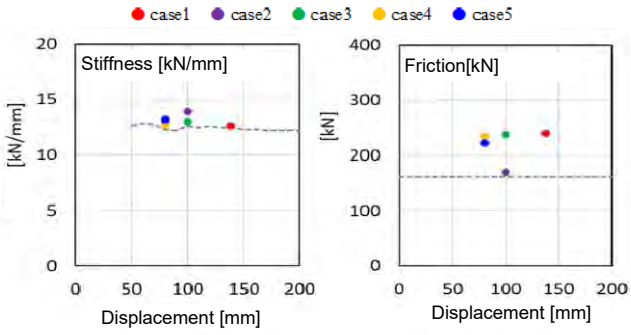

Fig.9 Evaluated stiffness and friction of base-isolated layer during static loading

5.2 Hysteresis characteristics of the base-isolated building based on vibration tests

Hysteresis loops of the free and forced vibration tests are shown in Figures 10 and 11, respectively; the vertical axis is a sum of the load-displacement relationship with a static loading of 138 mm forced displacement and inertial force, and the horizontal axis is the relative displacement of the base-isolated foundation layer. Figure 10 shows that energy is rapidly absorbed by the oil damper in the low-amplitude range when (a) the oil damper is present. The hysteresis shows a parallelogram shape when (b) the oil damper is not present and corresponds well with the static loading test results, with the influence of the isolated layer friction shown. The influence of the isolated layer friction independent of oil damper presence can be confirmed in Figure 11, and the intercept corresponds well with the load-displacement relationship during static loading conditions. Additionally, the hysteresis slope is larger than those of the load-displacement relationship of the static loading tests or the free vibration tests with no oil damper and is estimated to increase in the apparent stiffness of the base-isolated foundation layer because of the interference from friction in the low-amplitude range due to vibrations.

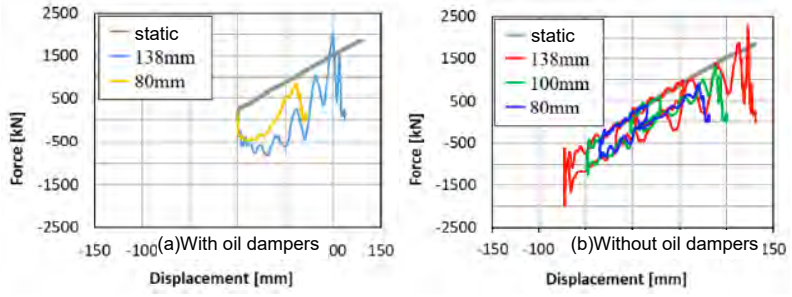

Fig.10 Hysteresis in free vibration tests

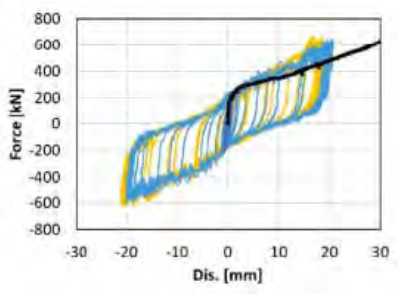

Fig.11 Hysteresis in forced vibration tests

5.3 Estimation of damping characteristics in the isolated layer due to free vibration waveform identification

The friction from the hysteresis in Section 5.2 to the isolated layer has a considerable influence on vibration characteristics, and it is thought from Section 5.1 that most of the friction in the isolated layer is due to CLB. Detailed investigations were conducted on the oil damper-excluded damping characteristics of the base-isolated foundation layer, based on the identification of base-isolated foundation layer waveforms from free vibration tests with no oil dampers conducted under rubber bearing + CLB conditions.

A model that combines viscous damping and frictional damping was used to identify these waveforms to simultaneously evaluate damping with different isolating layer characteristics. The equations of motion, which the friction force is considered to act opposite to the velocity direction, are used. The friction force is assumed to be due to CLB only, and characteristics were identified considering a CLB axial load ratio of 0.63.

Identification results are summarized in Table 2 and the identified waveform is shown in Fig.12. The modeled waveform results mostly corresponded with the measured waveforms up to the residual deformation following convergence of the vibrations. The modeled friction coefficient results corresponded with the standard values of 0.0039 for CLB, and it is thought that this prediction method which separately evaluated different damping characteristics was valid. The equivalent viscous damping coefficient due to the interference of viscous damping of rubber bearings and other setups was found to be 10-14%. The friction damping due to CLB was thought to correspond to approximately 10% of the equivalent viscous damping based on differences between this equivalent viscous damping coefficient and the damping coefficient in Table 1. Additionally, the natural period became shorter with smaller amplitude, and the vibration characteristics of the isolated layer were shown to be dependent on amplitude. The relationship between the identified natural period and the initial displacement of the free vibration corresponds to the period determined from the secant stiffness at the time of static loading and the building mass as shown in Fig.13.

Table 2 Estimated parameters with viscous damping and friction

Initial disp.	Initial vel.	Natural period	Damping	Friction coeff.
138 mm	2.95 cm/s	4.58 s	0.84	
100 mm	4.70 cm/s	4.01 s	0.21	
80 mm	1.19 cm/s	4.04 s	0.82	

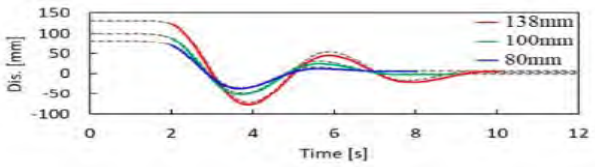

Fig.12 Identified waveforms – Solid : identified, Dashed : measured

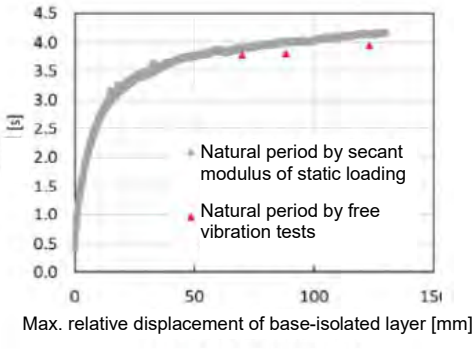

Fig.13 Natural period comparison

5.4 Damping characteristics of oil damper

The absolute axial strain of the rods during the free vibration tests as well as the relative displacement and velocity of the isolated layers are shown in Fig.14. Free vibration tests were conducted multiple times with an initial displacement of 130 mm, and reproducibility was confirmed. Damping force was measured at the rod of oil damper using strain gauges considering a value of 205 kN/mm^2 for the Young's modulus for a typical steel material, and 11,309.7 mm^2 for the rod cross-sectional area. Relationship of the velocity and damping force in the axial direction of the oil damper is shown in Fig.15. The damping force does not rise in the initial stages of free vibrational movement, is rapidly generated when the velocity surpasses approximately 0.05 m/s, and becomes proportional with velocity after the maximum velocity is crossed, with the slope corresponding well to the viscous damping coefficient of 2,500 kN/(m/s). The damping force acting in the east-west direction during the free vibration test due to the slanting direction of the oil damper is 0.34 times that of the oil damper in the east-west direction, and the damping force acting in the isolated layer during tests due to the oil damper is equivalent to 4.7 units' worth of oil dampers.

The damping coefficient calculated from this damping force 11,682 kN/(s/m), the average tangential stiffness of the base-isolated foundation layer is 13.1 kN/mm in Fig.9, and the obtained damping is approximately 64%. As shown in Table 1, the damping coefficients during the free vibration tests with and without the oil damper present were approximately 80% and 20%, respectively, and the damping due to oil dampers is thought to be approximately 60% using the difference of these two values, which approximately corresponds to the measured value of 64%.

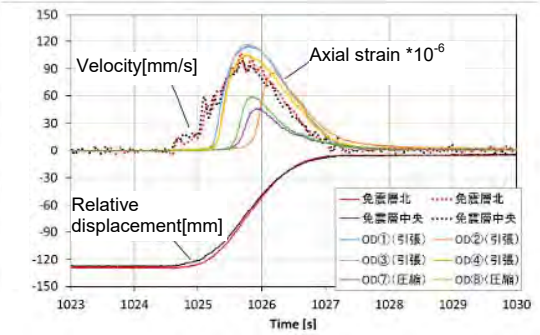

Fig.14 Axial strain of each oil damper with relative displacement and velocity of base-isolated layer

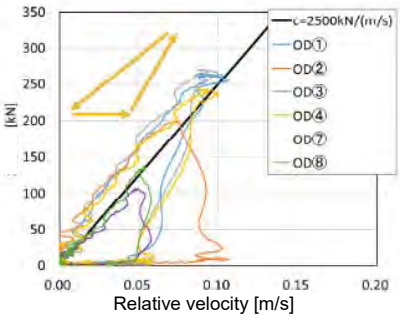

Fig.15 Relationship of damping force and relative velocity for each oil damper

6. Modeling of the Isolated Layer and Response Analysis

The restoring force characteristics of the base-isolated foundation layer were modeled in a trilinear manner based on hysteresis characteristics obtained from the forced vibration and static loading tests, and an elastic-plastic response analysis based on an SDOF model was obtained. Fig.16 shows the results of the analysis

where the input wave was set as the acceleration observed on the foundation of the subject building during the off the southeastern coast of Mie prefecture, Japan, earthquake on April 1, 2016. Results showed that the building response could be recreated within the low frequency components, below 1 Hz, of the acceleration Fourier spectra. Fig.17 shows the results of the analysis where the input wave was set as the simulated earthquake ground motion in the Nagoya region, which was created using the focal region of Nankai trough megathrust earthquakes published by the Central Disaster Prevention Council of the Japanese Cabinet Office. The acceleration of the upper structure greatly decreased, and sufficient aseismic performance was shown. Additionally, the responses of the design and the trilinear model were virtually identical, and a smaller influence due to non-linearity was confirmed during the high-amplitude response periods.

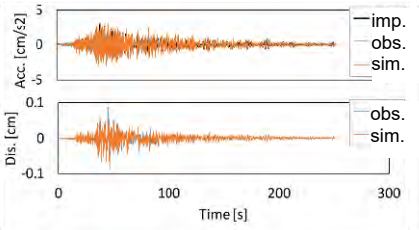

Fig.16 Observed and simulated response for small earthq.

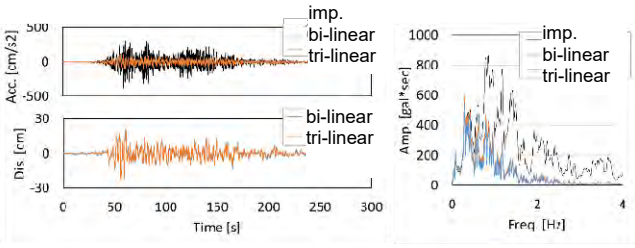

Fig.17 Inelastic simulation for large earthq.

7. Conclusion

It is thought that the vibration characteristics of base-isolated buildings can be clearly modeled, but there are virtually no examples where vibration characteristics or operating isolation device characteristics were investigated in detail based on measurements.

The present study conducted a detailed investigation on the vibration characteristics and isolation device characteristics of a base-isolated building based on vibration tests, using an actual base-isolated building with a varying vibration testing environment.

The development/improvement of the vibration test setup and the compiled monitoring methods/results based on continuous tests/observation will serve as useful documents for detailed analysis, including isolation device changes.

8. References

[1] Narusawa, K, Fukuwa, N, Tobita, J (2017): Design of a vibration test environment using an actual base-isolated building. *Journal of Structural Engineering*, **63B**, 251-258. (in Japanese).

[2] Fukuwa, N, Hirai, T, Tobita, J, Kurata, K(2016): Dynamic Response of Tall Buildings on Sedimentary Basin to Long-Period Seismic Ground Motion, *Journal of disaster research*, **11**(5), 857-869.

[3] Tobita, J(1996): Evaluation of Nonstationary Damping Characteristics of Structures under Earthquake Excitations, *Journal of Wind Engineering and Industrial Aerodynamics*, **59**(2,3), 283-298.